

Low-frequency Raman scattering in As_2S_3 glass former around the liquid–glass transition

This article has been downloaded from IOPscience. Please scroll down to see the full text article.

2003 J. Phys.: Condens. Matter 15 7651

(<http://iopscience.iop.org/0953-8984/15/45/004>)

View [the table of contents for this issue](#), or go to the [journal homepage](#) for more

Download details:

IP Address: 171.66.16.125

The article was downloaded on 19/05/2010 at 17:43

Please note that [terms and conditions apply](#).

Low-frequency Raman scattering in As_2S_3 glass former around the liquid–glass transition

N V Surovtsev¹, A M Pugachev¹, B G Nenashev² and V K Malinovsky¹

¹ Institute of Automation and Electrometry, Russian Academy of Sciences, Novosibirsk 630090, Russia

² United Institute of Geology, Geophysics, and Mineralogy, Russian Academy of Sciences, Novosibirsk 630090, Russia

Received 15 July 2003

Published 31 October 2003

Online at stacks.iop.org/JPhysCM/15/7651

Abstract

Low-frequency light scattering spectra of As_2S_3 glass former have been investigated over a temperature range of 300–712 K. Using the model of a damped oscillator, the parameters of the intensities of the boson peak and of the fast relaxation as well as the boson peak position and the relaxational time are extracted as a function of temperature. The temperature increase of the fast relaxation becomes more sharp above T_g and stabilizes at $T = 600$ K. By analogy with other glass formers it is suggested that the critical temperature T_c within the framework of the mode-coupling theory should be near 600 K for As_2S_3 . It was found that the damping parameter at T_c is the same for As_2S_3 and B_2O_3 ; an explanation of this coincidence is suggested. The boson peak is found to be present up to 712 K with almost the same strength as at low temperatures.

1. Introduction

Low-frequency ($1\text{--}100\text{ cm}^{-1}$) Raman scattering spectra of glasses have two contributions: vibrational spectrum (boson peak) and so-called quasielastic light scattering [1], the latter reflecting the contribution of fast relaxational processes in glassy substances [2–5]. While the vibrational spectrum follows the Bose statistics as the temperature increases, the peculiar feature of the fast relaxation spectrum is a more rapid increase in intensity with temperature. This feature usually serves as a way for extraction of the fast relaxation spectrum.

It was found that the increase in fast relaxation intensity with temperature becomes even more rapid above the glass transition temperature T_g , indicating that T_g is a particular point for the temperature dependence of the fast relaxation [6–12]. However, investigation of the fast relaxation and boson peak behaviour significantly above T_g is complicated by the contribution from very intense primary relaxation (α -relaxation) in their spectral range. As a result, the fast relaxation spectrum and boson peak hide in its high-frequency wing. This problem is more severe for fragile glasses. Strong glasses give more possibilities of investigating the

behaviour of the fast relaxation and boson peak above T_g in the absence or small influence of α -relaxation. Such a study was performed for the strong glass former B_2O_3 [13] and it was found that the boson peak exists even at temperatures much above T_g and also far above the melting temperature T_m . In this work, it was observed that the intensity of the fast relaxation becomes temperature-independent above a certain temperature, which is close to the critical temperature found in the analysis within the framework of the mode-coupling theory (MCT) [14]. Using the subtraction of α -relaxation, a similar change in the temperature dependence of the fast relaxation intensity was reported in some works [10, 12, 15]. However, it would be important to find other examples of such behaviour in glass forming systems where there is no need to apply the subtraction procedure. This would help to evidence that the change in the fast relaxation behaviour near T_c is a universal feature. In this respect, As_2S_3 glass former is an attractive case since its viscosity behaviour is closer to strong glasses [16] but its T_g is not too high, facilitating the investigation.

As_2S_3 glass is a widely studied glass and there is a long history of Raman investigations [17, 18], including the study of the low-frequency spectrum [19–22]. Various effects were studied for the low-frequency spectrum of As_2S_3 glass: preparation conditions [20, 21, 23], doping effect [24] and application of external stress [25]. However, studies of the temperature evolution of the low-frequency spectrum in As_2S_3 glass were restricted only by T_g . The darkening of this substance above T_g is the reason for this deficiency—there is a rise of the light absorption coefficient of As_2S_3 glass as the temperature increases [26]. The goal of the present work is to make up the deficiency by using excitation with a wavelength of $1.06 \mu m$ to study the low-frequency Raman spectrum of As_2S_3 glass former at high temperatures.

2. Experimental details

A polished cylinder of As_2S_3 bulk glass with a diameter of 12 mm was sealed in a silica tube with plate ends under vacuum conditions. A home-made oven was used for the high-temperature experiment.

Raman right-angle experiments were performed using a continuous YAG:Nd laser with a wavelength of 1064 nm, a typical power of 1 W, and a double-grating monochromator DFS-24 with a nitrogen cooled Ge-detector. Polarized and depolarized light scattering geometries were used in the experiment. Spectral slits of 2.2 cm^{-1} were used for recording spectra in the range $8\text{--}450 \text{ cm}^{-1}$ and smaller ones of 0.7 cm^{-1} in the range $3\text{--}30 \text{ cm}^{-1}$. The control method for the possible contribution from the elastic line to the low-frequency part of the spectrum was a comparison of the low-frequency spectra recorded with different spectral slits (more details in [27]). The Raman spectra obtained were free from the elastic line contribution down to $\sim 4 \text{ cm}^{-1}$. The highest temperature of the experiment was $T = 712 \text{ K}$, for which the thermal radiation from the sample causes problems with extraction of the Raman spectrum, and also strong reduction of the Raman signal was found for temperatures above 650 K, probably due to the increase in absorption of liquid As_2S_3 at such high temperatures.

3. Results

Figure 1 shows the polarized Raman scattering spectrum of As_2S_3 glass at three representative temperatures 293, 498 and 693 K in the reduced presentation,

$$I_n(\nu, T) = \frac{I(\nu, T)}{\nu(n+1)}, \quad (1)$$

eliminating the trivial temperature dependence for the vibrational spectrum ($n = 1/[\exp(h\nu/kT) - 1]$ is the Bose-factor). Assuming that the basic structure of the glass does not

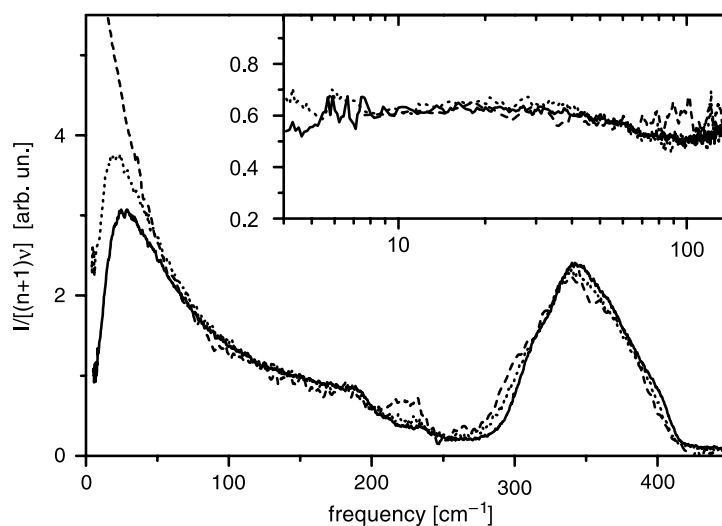


Figure 1. Polarized Raman spectrum of glassy As_2S_3 at $T = 293$ K (solid curve), 498 K (dotted curve) and 693 K (dashed curve). The inset shows the depolarization ratio at the same temperatures.

change significantly with temperature, the high-frequency mode near 350 cm^{-1} can be used for normalization of the Raman intensity. The band with the maximum lying near 25 cm^{-1} is the so-called boson peak. All spectra in figure 1 are similar for frequencies above $\sim 50\text{ cm}^{-1}$, evidencing the vibrational character of the spectra. The difference is the appearance of a small peak near 230 cm^{-1} for the spectrum at $T = 693\text{ K}$ which is attributed to the presence of As_4S_4 fragments due to the dissociation above the melting point [23]. This peak presents in the spectra for temperatures from 618 K and higher with approximately the same intensity as in figure 1. Estimation of the concentration of As_4S_4 fragments was done from the ratio of the intensities of the 230 and 350 cm^{-1} peaks and by using the results of [23]. The estimated content is about 5 mol%.

It is noticeable from figure 1 that there is the evidence of the boson peak with approximately the same intensity as at room temperature even at highest temperature of 693 K (higher than the melting point of As_2S_3 , for which values of $T_m = 585\text{ K}$ [26] and 572 K [28] have been reported). Also, it is worth noting that the vibrational spectrum does not undergo the dramatic spectral shift in the liquid state in comparison with the glassy state.

In contrast to the vibrational spectrum, the part of the spectrum below the boson peak maximum increases faster than the Bose-factor as the temperature increases (figure 1), revealing the fast relaxation contribution. In most previous works, it was found that the depolarization coefficient (the ratio of depolarized and polarized spectra) is approximately the same for the boson peak and fast relaxation [1, 3, 19]. In the case of glycerol [29], it was shown that this feature remains even at temperatures much above T_g . However, quite recently, a contrary result for As_2S_3 glass was found in the work [30]. In our opinion, this finding, which contradicts others, is related to improper suppression of the elastic line in the work [30]. In order to solve this controversial question, we checked the frequency and temperature behaviour of the depolarization ratio in our experiment, where the suppression of the elastic line was controlled by the method described in [27]. The inset shows the depolarization ratio of As_2S_3 at 293, 498 and 693 K. It is seen that our results support the universal feature of the low-frequency Raman spectrum of glass formers that the depolarization ratio of the fast relaxation spectrum is almost the same as at the boson peak maximum.

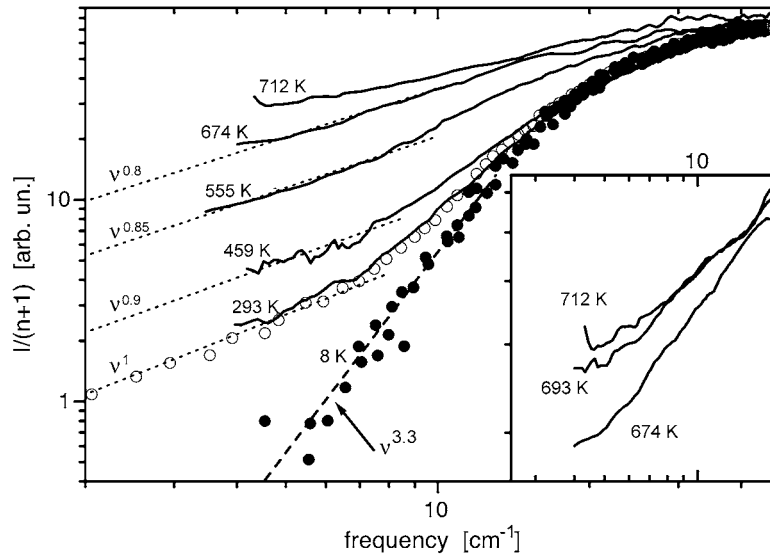


Figure 2. Susceptibility presentation of the low-frequency depolarized Raman spectra for glassy As_2S_3 at different temperatures (solid curves). The circles are data from [19]. The straight lines depict the power-law asymptotes at low frequencies. The inset shows the low-frequency part of the spectra at the highest temperatures in detail.

In order to emphasize the behaviour of the relaxational part of the low-frequency Raman spectrum, the experimental spectra in the susceptibility presentation

$$\chi''(\nu, T) \propto \frac{I(\nu, T)}{(n+1)} \equiv I_r \quad (2)$$

are shown in figure 2 in logarithmic scale. Two spectra at $T = 293$ and 8 K taken from the work [19] are added in figure 2. In the case where the fast relaxation spectrum corresponds to the exponential relaxation with a single relaxational time τ , the Debye spectrum is expected for the susceptibility:

$$\chi''(\nu) = \frac{\nu/\gamma}{1 + (\nu/\gamma)^2} \quad (3)$$

where $\gamma = 1/(2\pi\tau)$. Thus, the low-frequency asymptote $I_r \propto \nu$ is expected in the case of single relaxational time. As is seen from figure 2, up to 674 K the experimental low-frequency behaviour has an asymptote in the range $\nu^{0.8}-\nu^1$, meaning that the single relaxational time approximation is valid with good precision in the spectral range considered. At temperatures above 674 K, the α -relaxation wing comes into our spectral window (the inset of figure 2 shows this in detail) with the behaviour resembling the evolution of the low-frequency spectra of B_2O_3 when α -relaxation comes in [13].

4. Discussion

For extracting the quantitative characteristics of the fast relaxation and the boson peak, we used the model of a damped oscillator [2, 31–34]. This model naturally explains the same depolarization ratio for the boson peak and the quasielastic spectrum [1–3], the same magnitude of the coupling coefficient [35], and the same damping coefficient around the boson peak and for acoustic modes [5, 33, 36]. Moreover, it was shown recently that the direct mechanism is

not able to explain the behaviour of the high-frequency part of the quasielastic excess [37]. In the model of a damped oscillator, the fast relaxation is manifested in light scattering spectra as a relaxational part of the response of boson peak vibrations. For the case of exponential relaxation with single relaxational time, the low-frequency Raman spectrum is written as [34]

$$I_n(T, \nu) = \frac{2}{\pi} \int_0^\infty \frac{I_n^0(T, \Omega) \Omega^4 \delta_0^2 \gamma / (\nu^2 + \gamma^2)}{(\Omega^2 - \nu^2 - \delta_0^2 \gamma^2 \Omega^2 / (\nu^2 + \gamma^2))^2 + (\delta_0^2 \gamma \nu \Omega^2 / (\nu^2 + \gamma^2))^2} d\Omega \quad (4)$$

where $I_n^0(T, \Omega)$ is the true vibrational spectrum at a temperature T in the absence of relaxation. The parameter δ_0^2 reflects the strength of the fast relaxation and has the following relationship with $g(T)$ defined as the ratio between the integral over the quasielastic spectrum and the integral over the vibrational spectrum [34]:

$$g(T) = \delta_0^2(T) / (1 - \delta_0^2(T)). \quad (5)$$

The vibrational spectrum at zero temperature can be found by assuming that the influence of the fast relaxation is negligible at sufficiently low temperatures. Thus, the spectrum at the lowest temperature (8 K) shown in figure 2 can be taken as the vibrational spectrum at zero temperature. It is seen that this spectrum has the low-frequency asymptote close to $I_r(\nu) \propto \nu^3$, which is typical for the Raman spectra of glasses at low enough temperatures where the fast relaxation can be neglected.

We assumed that the evolution of the pure vibrational spectrum as the temperature increases results in its quasiharmonic shift, which can be described by the relation

$$I_n^0(T, \nu) = I_n^0(T = 0, \nu\eta)\eta^2. \quad (6)$$

Here the parameter η describes the quasiharmonic shift of the vibrational spectrum. The amplitude correction in equation (6) was found under the following assumptions:

- (i) the coupling coefficient of the vibrational spectrum $C(\nu)$ in the Shuker–Gammon formula [38] is proportional to frequency, that is valid in the spectral range of the boson peak in the case of As₂S₃ glass [39];
- (ii) the magnitude of $C(\nu)$ is a function of frequency and does not depend on temperature;
- (iii) the integral over the vibrational density of states is a temperature-independent constant.

In the fitting procedure, we used a free fitting parameter A :

$$I_n^0(T, \nu) = AI_n^0(T = 0, \nu\eta)\eta^2. \quad (7)$$

The parameter A is equal to 1 if the assumptions (i)–(iii) are valid. Assumption (ii), about the temperature evolution of the vibrational spectrum, can be changed to state instead: the magnitude of $C(\nu)$ is a function of a particular vibration and shifts with temperature together with the frequency shift of the vibration. In this case, equation (7) takes the form

$$I_n^0(T, \nu) = AI_n^0(T = 0, \nu\eta)\eta. \quad (8)$$

We used equations (4) and (7) with four parameters, A , η , δ_0^2 and γ , for fitting the experimental spectra up to the temperature 674 K where the single relaxational time approximation is valid (figure 2). The case of equation (8) is obtained by simple rescaling of the parameter A . Figure 3 shows the experimental and curve fits for three representative temperatures.

The parameter δ_0^2 is the only parameter responsible for the intensity of the fast relaxation which is related to the relative portion of the relaxation spectrum via equation (5). In figure 4, the results for the temperature dependence of the parameter $g(T)$ are shown by circles. It is seen that the most drastic temperature dependence of $g(T)$ is at $T > T_g$. In order to visualize the evolution of $g(T)$ below T_g , the logarithmic scale is used in figure 4(b). To

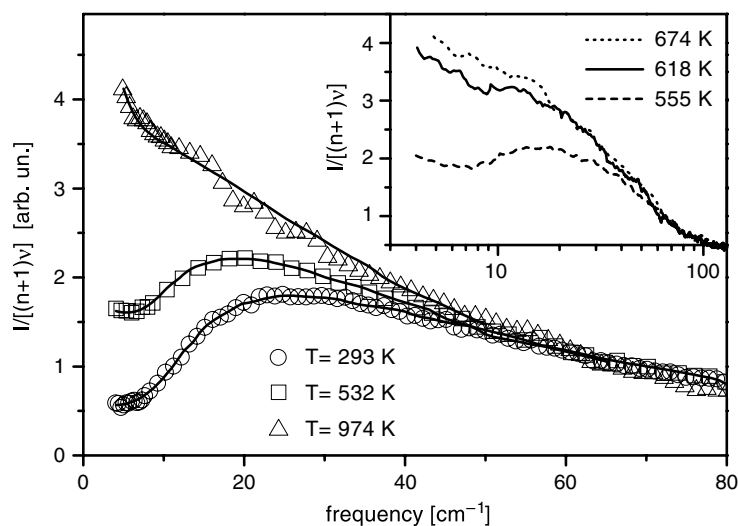


Figure 3. Representative low-frequency depolarized Raman spectra of As_2S_3 at three temperatures and their fit using equations (4) and (7). Inset shows three Raman spectra of As_2S_3 at $T = 555$, 618 and 674 K with a logarithmic scale for the frequency axis.

extend our temperature range and to cross-check our experimental data, we have also fitted the low-frequency depolarized Raman spectra published previously by other research groups: [19] ($T = 296$ K), [22] ($T = 100, 192, 293, 390$ K) and [40] ($T = 54$ K). The results for the parameter $g(T)$ are shown in figure 4, which demonstrate good agreement with our data and extend the temperature range. The open triangles in figure 4 show the results for the integrated intensity of the fast relaxation spectrum found in [3] within the framework of the superposition of the boson peak and the fast relaxation spectrum (which is a good approximation if δ_0^2 is small [34]). The results of [3] were scaled to $g(T)$ at room temperature.

From figure 4 it is seen that, starting from the lowest temperature, the intensity of the fast relaxation spectrum increases with T , becoming about ten times more intense at T_g than at $T = 54$ K. This rather gradual growth of $g(T)$ as the temperature increases changes to a sharper increase in the range $T_g - 1.3T_g$. In figure 4, $T_g = 461$ K for As_2S_3 is used. Note that there is a wide scatter in this magnitude of As_2S_3 glass—from 440 K [28] to 478 K [22]. We used the value taken from [41] where T_g is defined for standard conditions—the cooling at 5 K min^{-1} of a well-annealed sample of pure As_2S_3 .

The sharp increase of the fast relaxation intensity is arrested in the temperature range near 600 K (figure 4) in full agreement with the results found previously in [10, 12, 13, 15]. The weak temperature dependence of the fast relaxation is documented up to $T = 674$ K and the α -relaxation wing comes into our spectral window at higher temperatures. In order to demonstrate that the change of the temperature increase of the fast relaxation intensity near 600 K is not an occasional artifact of the fitting procedure, in the inset of figure 3 the spectrum at $T = 618$ K is compared with two other spectra. One of these is measured at a temperature about 60 K higher and the other about 60 K lower (a logarithmic scale is used for frequency axis to visualize the low-frequency part and the behaviour at the high-frequency part of the boson peak). It is seen from this figure that the two spectra at the higher temperatures are much closer to each other than to the spectrum at lower T , supporting the idea that the temperature increase of the fast relaxation is much lower in the range $T > 618$ K.

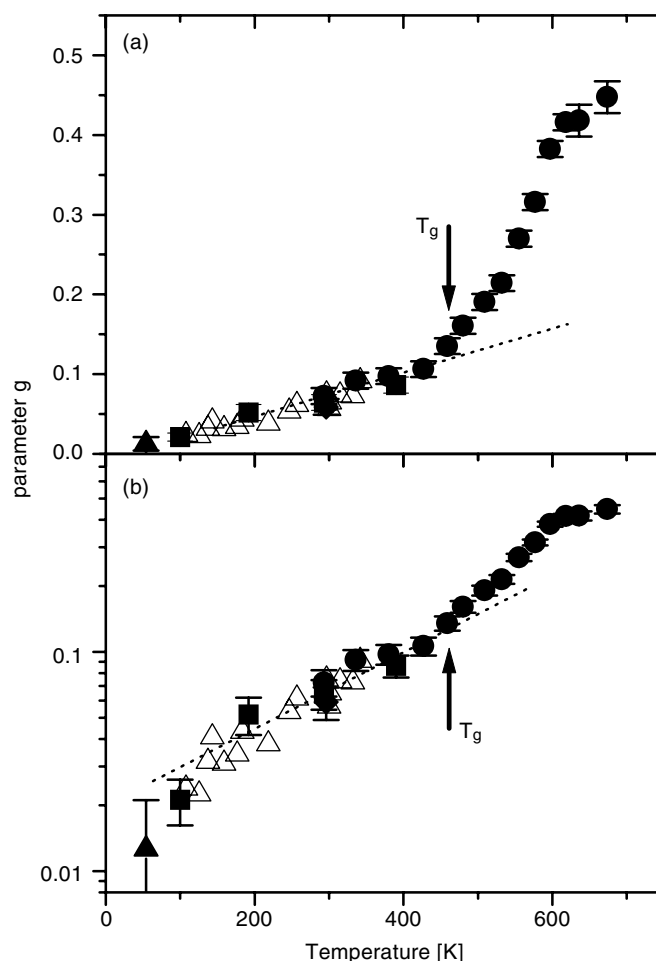


Figure 4. Temperature dependence of the fitting parameter g in linear (a) and semilogarithmic presentation (b). The circles are from fits of spectra recorded in the present work, the filled diamond (at 296 K) from [19], the squares from [22] and the solid triangle from [40]. The open triangles show the total intensity of the relaxational spectrum from [3] scaled to the magnitude of the parameter g at room temperature. The dotted lines are guides for the eyes.

As_2S_3 is only the second substance for which this observation has been made without the subtraction of the α -relaxation wing. It is especially important because B_2O_3 glass, the first substance that unambiguously demonstrated this behaviour, shows significant changes in its structure at temperatures above T_g —the concentration of the boroxol rings, B_3O_3 , decreases at high temperatures [42]. However, as was evidenced above, there are some structural changes also for the As_2S_3 melt, related to the formation of As_4S_4 and S_2 [23]. So, one could argue that the effect of the stabilization of the temperature increase of the fast relaxation is related to the modification in the structure of the melt. Nevertheless, we believe that this effect has a minor influence for the fast relaxation behaviour in the range 600–700 K. The main arguments are following: the estimated small concentration of fragments of As_4S_4 and the reversed role of defects—usually the appearance of structural defects leads to an increase of the fast relaxation intensity, not to suppression (for example, [43]).

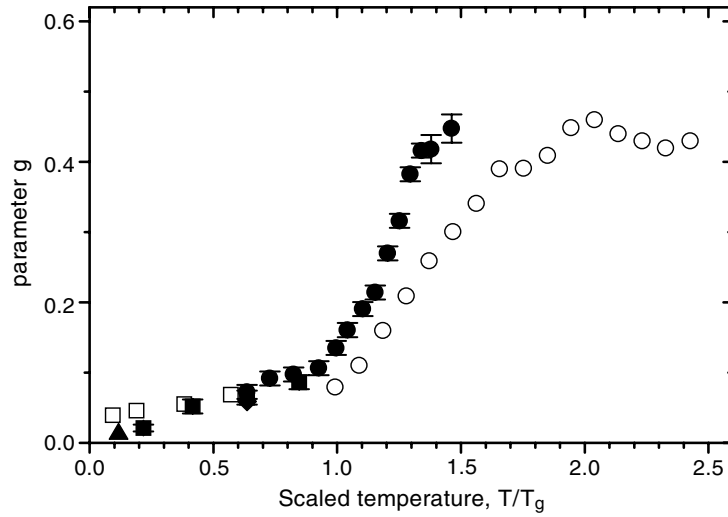


Figure 5. $g(T)$ for As_2S_3 and B_2O_3 glass formers scaled by glass transition temperature. The symbols for As_2S_3 are the same as in figure 4, the open circles are results from [13] and the open squares are the results of fits for spectra from [44].

In previous studies, the arrest of the fast relaxation growth was found near T_c —the critical temperature within the framework of MCT analysis [10, 12, 13, 15]. Unfortunately, to our knowledge, there are no estimations of T_c for As_2S_3 glass former. Assuming that the general correlation is also valid for As_2S_3 , the results of the present investigation allow us to estimate T_c of As_2S_3 to be around 600 K.

In figure 5, the parameter $g(T)$ is shown for As_2S_3 and B_2O_3 versus the temperature scaled by T_g . Qualitative similarity of the fast relaxation intensity behaviour for these two glass formers is seen from this figure. The difference between the behaviours of two substances is the magnitude of the temperature range with the sharp increase of $g(T)$ —it is shorter for As_2S_3 reflecting that this substance is more fragile than B_2O_3 (the ratio T_c/T_g is higher for stronger glass formers [45, 46]). It is remarkable that the arrest of the fast relaxation growth occurs at approximately the same value of $g(T) = 0.4\text{--}0.45$ (corresponding to $\delta_0^2 \approx 0.3$). It is not clear at the moment whether this is an occasional coincidence or this reflects some general tendency.

However, we will argue that a fixed value of $\delta_0^2 \approx 0.3$ could be expected at T_c within the framework of some qualitative speculations. Let us consider the presentation of the glass structure as an inhomogeneous structure [47, 48]. In this simplified case, the boson peak appears as fundamental modes of nanoclusters constituting the glass structure and reflects their distribution. Correspondingly, the maximum of the boson peak reflects the characteristic nanocluster of a glass former. T_c is often interpreted as a temperature at which a relaxing group (an atom) escapes from a cage formed by its neighbours [46], so this temperature means the temperature at which this cage freezes when the glass former is cooled. Within the framework of the inhomogeneous glassy structure, this freezing could be related to the change in the nanocluster dynamics or, in other words, in the dynamic of the boson peak vibration. Denote the position of the boson peak maximum as Ω_{bp} . The width of this vibration Γ_{bp} (full width at half maximum) can be found from equation (4)

$$\Gamma_{\text{bp}} \approx \frac{\delta_0^2 \gamma \Omega_{\text{bp}}^2}{\Omega_{\text{bp}}^2 + \gamma^2} \quad (9)$$

where relatively weak damping of the boson peak maximum is assumed:

$$\frac{\delta_0^2 \gamma \Omega_{\text{bp}}}{\Omega_{\text{bp}}^2 + \gamma^2} \ll 1, \quad \frac{\delta_0^2 \gamma^2}{\Omega_{\text{bp}}^2 + \gamma^2} \ll 1. \quad (10)$$

In the spirit of the present discussion, a particular ratio between Γ_{bp} and Ω_{bp} corresponds to T_c . We suggest a dynamical analogue of the Lindemann criterion of melting [49]. Application of the Lindemann criterion to the explanation of the universalities of the glass former characteristics has been suggested before [46]; in this case, T_c corresponds to the temperature for which the mean square atomic displacement is 0.12–0.15 of the interatomic distance. Just by analogy, we suggest the dynamic analogue of the Lindemann criterion—at T_c

$$\Gamma_{\text{bp}}/\Omega_{\text{bp}} \approx 0.12. \quad (11)$$

In [50] the empirical relation between γ of the fast relaxation and Ω_{bp} was proposed. In contrast, we use the definition of Ω_{bp} as a maximum position of the vibrational density of states divided by squared frequency, which leads to the correction of the empirical relation of [50] into the approximate form

$$\gamma \approx \Omega_{\text{bp}}/2. \quad (12)$$

Using equations (11) and (12), one can find from equation (9) that $\delta_0^2 \approx 0.3$ at T_c . Thus, this simple consideration allows us to pose the hypothesis that the agreement of δ_0^2 at T_c for the two glass formers shown in figure 5 is not occasional but reflects more fundamental reasons.

The temperature dependences of other parameters found from the fitting of the experimental low-frequency Raman spectra of As₂S₃ are shown in figure 6. The width of the relaxational spectrum (figure 6(b)) does not show a discernible temperature dependence, remaining close to 8 cm⁻¹. This behaviour is common for fast relaxation of glasses (see, for example, [7, 34, 51, 52]) and the present work allows us to extend this feature also above T_g .

Figure 6(a) shows the temperature evolution of the parameter A , reflecting the total intensity of the low-frequency Raman spectra, which is expected to be temperature-independent if the low-frequency vibrations or their Raman-vibration coupling strengths have no abrupt changes above T_g . The results for the assumptions of both equations (7) and (8) are shown in this figure. From figure 6(a), one can conclude that the parameter A is temperature-independent with good precision ($\sim 15\%$). Therefore, the boson peak vibrations remain in the liquid state with the same intensity although more damped than in the deeply glassy state. A similar feature is expected for the B₂O₃ glass from the result of [53] where it was shown that the total integrated intensity of the Bose-factor corrected low-frequency spectrum is temperature-independent up to about 1100 K. The advantage of the present study is the use of the high-frequency mode for the normalization procedure, which allows us to avoid the ambiguity of the direct intensity normalization.

In previous studies, the opposite statements about the boson peak intensity in the liquid state were also suggested. For example, the authors of [54] concluded that the boson peak intensity for orthoterphenyl (OTP) decreases with increasing temperature above $T_g = 244$ K and vanishes near $T = 320$ K ($T_m = 329$ K). Rather than the principal difference between the different glass formers holding, we assume that the contradiction with [54] is due to the absence of the high-frequency mode intensity normalization in the work [54] and (probably more important) the smearing of the low-frequency spectrum by the α -relaxation wing, which occurs at lower temperatures for more fragile OTP glass former. Let us note that there are no theoretical expectations of the disappearance of the boson peak in the liquid state of the glass former. Indeed, a typical relaxational time of α -relaxation responsible for the

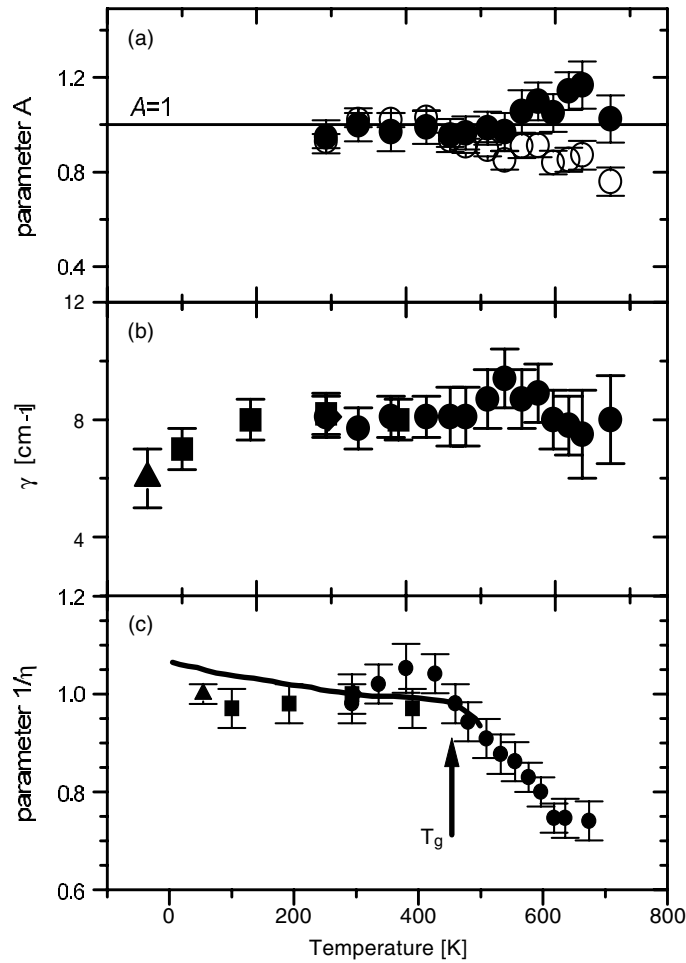


Figure 6. Temperature dependence of the fitting parameters (the symbols are the same as in figure 4): (a) parameter A , where the open circles corresponds to equation (8) and solid ones to equation (7), (b) parameter γ and (c) parameter $1/\eta$. The solid curve is the temperature dependence of the sound velocity for As_2S_3 glass scaled to unity at room temperature (data from [22]).

local structure fluctuations and reconstructions is usually much lower than the period of the boson peak vibrations. Therefore, the boson peak vibrations exist within the instantaneous structure of the glass former where α -relaxation is effectively frozen. Thus, the eigenfrequency and instantaneous wavefunction of the boson peak vibrations are determined solely by the instantaneous structure. On the other hand, it is well known that the instantaneous structure of glass formers is almost the same for the liquid and glassy states [55]. Hence, the instantaneous boson peak vibrations are the same for the liquid and glassy states. The difference appears in time evolution of the wavefunction due to different anharmonic (relaxational) interaction in different states, leading to vibrational damping, which can be taken into account in a standard manner such as in equation (4) [56].

The temperature dependence of the parameter $1/\eta$, responsible for the quasiharmonical shift of the vibrational spectrum, is shown in figure 6(c). From this figure, it is seen that the vibrational spectrum does not undergo any noticeable quasiharmonical shift below T_g ; this

shift starts at T_g and has a tendency to stop at $T > 600$ K. Note that the temperature of stabilization of the boson peak position is the same as the temperature of the arrest of the fast relaxation intensity growth (figure 4). The decrease in the boson peak frequencies at $T > T_g$ reflects the decrease in the sound velocity (figure 6(c)), which seems to be the general rule for glass formers [9]. Note that a similar observation can be made for B₂O₃ glass former—the decrease in the boson peak maximum at $T > T_g$ stops in the range of 700–750 K [53]; also this behaviour has a counterpart in the behaviour of the sound velocity [57, 58].

Our results for the boson peak position do not support the extrapolation of the low-frequency Raman data of As₂S₃ at $T < 478$ K proposed in [20], which predicts zeroing of the boson peak position at $T = 588$ K. However, for some other substances, it was also suggested that the position of the boson peak tends to zero frequency at sufficiently high temperatures [31, 32, 59]. The difference between substances studied in these works (zinc chloride, OTP, m-TCP, and glycerol) and As₂S₃ and B₂O₃ glass formers is the greater influence on the α -relaxation spectrum in the spectral range close to the boson peak maximum. In [59], it was pointed out that the temperature of the apparent zeroing of the boson peak position cannot be considered to be T_c as was suggested before.

5. Conclusion

A study of the low-frequency Raman spectrum for As₂S₃ glass former in the range $T = 300$ – 712 K is presented. It was found that the temperature growth of the fast relaxational spectrum mimics the behaviour found previously for B₂O₃ and for some other glass formers within the framework of some analysis: at the glass transition temperature ($T_g = 461$ K) there is sharp increase in the rate of the temperature growth of the fast relaxation. This growth is arrested at 600 K, and the fast relaxational spectrum does not show remarkable growth, at least up to 674 K. By analogy with B₂O₃ glass, it was suggested that $T = 600$ K corresponds to T_c within the framework of MCT. It was found that the damping parameter reflecting the fast relaxation intensity is about the same at T_c for As₂S₃ and B₂O₃ glasses. A hypothesis that this agreement could reflect the general rule is proposed and discussed.

In contrast to previous extrapolations of low-temperature spectra, it was shown unambiguously that neither intensity nor spectral position of the boson peak maximum are zeroing in the temperature range of the study, with the highest temperature significantly exceeding the melting point ($T_m \sim 580$ K).

Acknowledgments

The authors are grateful to I A Sokolov for the assistance during the experimental work. The authors thank the referee for addressing their attention to the problem of the high-temperature dissociation of As₂S₃ and to the alternative interpretation of the high-temperature stabilization of the fast relaxation increase. This work was supported by RFBR Grant No 02-02-16112.

References

- [1] Jäckle J 1981 *Amorphous Solids: Low-Temperature Properties* ed W A Phillips (Berlin: Springer) p 135
- [2] Winterling G 1975 *Phys. Rev. B* **12** 2432
- [3] Gochiyayev V Z and Sokolov A P 1989 *Sov. Phys.—Solid State* **31** 557
- [4] Surovtsev N V, Wiedersich J A H, Novikov V N, Rössler E and Sokolov A P 1998 *Phys. Rev. B* **58** 14888
- [5] Wiedersich J, Adichtchev S V and Rössler E 2000 *Phys. Rev. Lett.* **84** 2718
- [6] Krüger M, Soltwisch M, Petscherizin I and Quitmann D 1992 *J. Chem. Phys.* **96** 7352
- [7] Krüger M, Kisliuk A, Sokolov A, Soltwisch M and Quitmann D 1993 *J. Phys.: Condens. Matter* **5** B127
- [8] Lorösch J, Couzi M, Pelous J, Vacher R and Lévassieur A 1984 *J. Non-Cryst. Solids* **69** 1
- [9] Terki F, Levelut C, Prat J L, Boissier M and Pelous J 1997 *J. Phys.: Condens. Matter* **9** 3955

- [10] Wiedersich J, Surovtsev N V and Rössler E 2000 *J. Chem. Phys.* **113** 1143
- [11] Ribeiro M C C, de Oliveira L F C and Gonçalves N S 2001 *Phys. Rev. B* **63** 104303
- [12] Adichtchev S V, Benkhof S, Blochowicz T, Novikov V N, Rössler E, Tschirwitz C and Wiedersich J 2002 *Phys. Rev. Lett.* **88** 055703
- [13] Brodin A, Börjesson L, Engberg D, Torrel L M and Sokolov A P 1996 *Phys. Rev. B* **53** 11511
- [14] Götze W and Sjögren L 1992 *Rep. Prog. Phys.* **55** 241
- [15] Rössler E, Novikov V N and Sokolov A P 1997 *Phase Transit.* **63** 201
- [16] Angell C A 1988 *J. Non-Cryst. Solids* **102** 205
- [17] Ward A T 1968 *J. Phys. Chem.* **72** 4133
- [18] Kobliska R J and Solin S A 1973 *Phys. Rev. B* **8** 756
- [19] Nemanich R J 1977 *Phys. Rev. B* **16** 1655
- [20] Kawamura H, Fukumasu F and Hamada Y 1982 *Solid State Commun.* **43** 229
- [21] Malinovsky V K and Sokolov A P 1986 *Solid State Commun.* **57** 757
- [22] Yasuoka H, Onari S and Arai T 1986 *J. Non-Cryst. Solids* **88** 35
- [23] Mamedov S, Kisliuk A and Quitmann D 1998 *J. Mater. Sci.* **33** 41
- [24] Tikhomirov V K, Santos L F, Almeida R M, Jha A, Kobelke J and Scheffler M 2001 *J. Non-Cryst. Solids* **284** 198
- [25] Kastrissios D Th, Papatheodorou G N and Yannopoulos S N 2001 *Phys. Rev. B* **64** 214203
- [26] Zakis J R and Fritzsche H 1974 *Phys. Status Solidi b* **64** 123
- [27] Surovtsev N V, Batalov A E, Kulakov V I, Nikolaev R K, Pugachev A M and Malinovsky V K 2002 *Phys. Rev. B* **66** 205412
- [28] Tanaka K 1985 *Solid State Commun.* **54** 867
- [29] Kojima S 1993 *Phys. Rev. B* **47** 2924
- [30] Yannopoulos S N and Papatheodorou G N 2000 *Phys. Rev. B* **62** 3728
- [31] Gochiyaev V Z, Malinovsky V K, Novikov V N and Sokolov A P 1991 *Phil. Mag.* **B 63** 777
- [32] Sokolov A P, Kisliuk A, Quitmann D, Kudlik A and Rössler E 1994 *J. Non-Cryst. Solids* **172–174** 138
- [33] Sokolov A P, Novikov V N and Strube B 1997 *Europhys. Lett.* **38** 49
- [34] Novikov V N, Sokolov A P, Strube B, Surovtsev N V, Duval E and Mermet A 1997 *J. Chem. Phys.* **107** 1057
- [35] Sokolov A P, Buchenau U, Steffen W, Frick B and Wischnewski A 1995 *Phys. Rev. B* **52** R9815
- [36] Novikov V N, Surovtsev N V, Wiedersich J, Adichtchev S, Kojima S and Rössler E 2002 *Europhys. Lett.* **57** 838
- [37] Novikov V N, Surovtsev N V and Kojima S 2001 *J. Chem. Phys.* **115** 5278
- [38] Shuker R and Gammon R W 1970 *Phys. Rev. Lett.* **25** 222
- [39] Surovtsev N V and Sokolov A P 2002 *Phys. Rev. B* **66** 054205
- [40] Sokolov A P, Kisliuk A, Quitmann D and Duval E 1993 *Phys. Rev. B* **48** 7692
- [41] Málek J 1998 *Thermochim. Acta* **311** 183
- [42] Hassan A K, Torell L M, Börjesson L and Doweidar H 1992 *Phys. Rev. B* **45** 12797
- [43] Surovtsev N V, Mermet A, Duval E and Novikov V N 1996 *J. Chem. Phys.* **104** 6818
- [44] Surovtsev N V, Wiedersich J A H, Duval E, Novikov V N, Rössler E and Sokolov A P 2000 *J. Chem. Phys.* **112** 2319
- [45] Rössler E, Sokolov A P, Kisliuk A and Quitmann D 1994 *Phys. Rev. B* **49** 14967
- [46] Novikov V N and Sokolov A P 2003 *Phys. Rev. E* **67** 031507
- [47] Duval E, Bouknter A and Achibat T 1990 *J. Phys.: Condens. Matter* **2** 10227
- [48] Sokolov A P, Kisliuk A, Soltwisch M and Quitmann D 1992 *Phys. Rev. Lett.* **69** 1540
- [49] Lindemann F A 1911 *Z. Phys.* **11** 609
- [50] Novikov V N 1997 *Phys. Rev. B* **55** R14685
- [51] Carini G, Federico M, Fontana A and Saunders G A 1993 *Phys. Rev. B* **47** 3005
- [52] Carini G, D'Angelo G, Tripodo G, Fontana A, Leonardi A, Saunders G A and Brodin A 1995 *Phys. Rev. B* **52** 9342
- [53] Walrafen G E, Hokmabadi M S, Krishnan P N, Guha S and Munro P G 1983 *J. Chem. Phys.* **79** 3609
- [54] Steffen W, Zimmer B, Patkowski A, Meier G and Fischer E W 1994 *J. Non-Cryst. Solids* **172–174** 37
- [55] Elliott S R 1990 *Physics of Amorphous Materials* (London: Longman)
- [56] Novikov V N 1998 *Phys. Rev. B* **58** 8367
- [57] Grimsditch M, Bhadra R and Torell L M 1989 *Phys. Rev. Lett.* **62** 2616
- [58] Youngman R E, Kieffer J, Bass J D and Duffrène L 1997 *J. Non-Cryst. Solids* **222** 190
- [59] Lebon M J, Dreyfus C, Li G, Aouadi A, Cummins H Z and Pick R M 1995 *Phys. Rev. E* **51** 4537